The fabrication of a flexible and portable sensor based on home-made laser-induced porous graphene electrode for the rapid detection of sulfonamides

Yifang Zeng, Qian Li, Wenjun Wang, Yangping Wen, Kunxia Ji, Xiaoxue Liu, Pianpian He, Bruno Campos Janegitz, Kaijie Tang

PII: S0026-265X(22)00726-3
DOI: https://doi.org/10.1016/j.microc.2022.107898
Reference: MICROC 107898

To appear in: *Microchemical Journal*

Received Date: 28 March 2022
Revised Date: 12 August 2022
Accepted Date: 17 August 2022

Please cite this article as: Y. Zeng, Q. Li, W. Wang, Y. Wen, K. Ji, X. Liu, P. He, B. Campos Janegitz, K. Tang, The fabrication of a flexible and portable sensor based on home-made laser-induced porous graphene electrode for the rapid detection of sulfonamides, *Microchemical Journal* (2022), doi: https://doi.org/10.1016/j.microc.2022.107898

The fabrication of a flexible and portable sensor based on home-made laser-induced porous graphene electrode for the rapid detection of sulfonamides

Yifang Zeng[a,b], Qian Li[a,b], Wenjun Wang[a], Yangping Wen[b*], Kunxia Ji[a,b], Xiaoxue Liu[a,b], Pianpian He[a,b], Bruno Campos Janegitz[c], Kaijie Tang[a*]

[a]College of Food Science and Engineering, Jiangxi Agricultural University, Nanchang 330045, People's Republic of China

[b]Institute of Functional Materials and Agricultural Applied Chemistry, Jiangxi Agricultural University, Nanchang 330045, People's Republic of China

[c]Department of Nature Sciences, Mathematics and Education, Federal University of São Carlos, 13600-970, Araras, SP, Brazil

*Corresponding author:

E-mail: wenyangping1980@jxau.edu.cn (Y. Wen), tkjie999@sina.com (K. Tang).

Abstract

A smartphone-based wireless electrochemical sensor for portable and fast detection of sulfonamides (SAs) using home-made flexible integrated three-electrode of laser-induced porous graphene (LIPG) modified with two-dimensional hexagonal boron nitride (2D h-BN) as working electrode was developed. The flexible integrated three-electrode of LIPG was prepared by direct laser-writing technique on polyimide (PI) film. The reference electrode was handmade by casting a silver and silver chloride ink on the surface of the LIPG. With excellent electrochemical performance, the pocket, disposable, cost-effective, flexible three-electrode constructed a novel sensing platform to detect sulfamethoxazole (SMZ) at a lower electrochemical oxidation potential of 0.56 V. The developed sensor displayed a good linear range from 0.5 to 362.5 μM, a low limit of detection was 0.011 μM and satisfactory recovery in the range of 97.5% - 101.3% in milk and lake water. This sensor was also applied for the detection of four other SAs (sulfanilamide, sulfapyridine, sulfadimidine, sulfisoxazole). This work will be valuable to the development of a simple, fast sensing platforms for outdoor detection and online monitoring in food safety and environmental safety areas.

Keywords: Flexible sensor; Integrated three-electrode; Sulfonamides; Laser-induced porous graphene; Hexagonal boron nitride

1. Introduction

Sulfonamides (SAs), a broad-spectrum antibacterial drug with *p*-aminobenzene sulfonamide, are widely used around the world due to their stable chemical properties, convenient use and low price. But a large amount of production and excessive or irrational application of antibiotics has induced various risk in food contamination and environmental pollution. Sulfamethoxazole (SMZ), one of the representatives of sulfonamides antibiotics, plays an important role in preventing and treating infections. As a highly persistent pollution, SMZ has large toxicological effects in animal-derived food and aquatic environment [1,2], and it is one of three sulfonamides (the other two are sulfisoxazole and sulfamethazine) have been classified as a Category 3 carcinogen by the World Health Organization. When exposing to a low level of antibiotics over a long period of time, humans may suffer from the risk of antibiotic resistance and even thyroid cancer [3,4]. In China, European Union and other countries, the safe limit for sulfonamide residues should not exceed 100 $\mu g \cdot kg^{-1}$ in edible animal tissue and should not exceed 25 $\mu g \cdot kg^{-1}$ in milk. Therefore, the development of effective and convenient methods to detect residual antibiotics from food and water is imperative [5].

SMZ and other SAs have normally been detected by laboratory-based analytical techniques, such as chromatography and coupled to other methods, fluorescence techniques [6-8], which can provide good qualitative or quantitative information. However, these techniques require expensive and bulky equipment, a lot of time in complicated sample preparation and are limited to use in the laboratory. It cannot

meet the requirements of the trending of simple, quick, portable, and low-cost tests for antibiotic residues analysis. Electrochemical sensors are the most promising method due to its low cost, simple operation, and fast response in trace analysis [9-13]. In recent years, electrochemical sensors are developing towards miniaturization, integration, networking and intelligence, which has been used for trace analysis of hazardous substances [14-18].

With the development of portable devices, the smart and miniaturized sensors for on-site fast detecting have become one of the hotspots in the field of sensing. However, the conventional rigid electrodes cannot meet this requirement, hence the research of flexible and pocket electrode has attracted extensive attention in the worldwide. A flexible electrode based on laser-induced porous graphene (LIPG) using laser direct writing technology has been studied in our laboratory for several years, and it had successfully deployed in electrochemical sensors for practical usage in evaluation of fish freshness, intelligent analysis of phytohormone and SAs [19-23]. But so far, the research on LIPG is only limited to the preparation and application of the flexible working electrode, while this study focused on the flexible integrated three-electrode (working electrode, reference electrode and counter electrode) based on LIPG is few reported. Although commercial screen-printed electrodes (SPCE) as three-electrode system combined with portable sensors and smartphone are currently available for convenient detection of antibiotics including SAs [24,25], the high limit of detection (LOD) and high electrochemical oxidation potential for sulfamethoxazole is not ideal [26,27]. The three-electrode system is still in its infancy, its tremendous

application foreground in portable sensing analysis and outdoor detection has great research value. In our study, a flexible integrated three-electrode was prepared on polyimide (PI) film using direct laser-writing technique, the working electrode (can be chemically modified) and the auxiliary electrode is bare LIPG, the reference electrode was handmade by casting silver and silver chloride ink on the porous graphene conducting track. The homemade flexible integrated three-electrode can fit perfectly with a portable mini-workstation and can be connected to a smartphone via Bluetooth. It not only replaced glassy carbon electrode coupled with both traditional large-scale workstation and tablet computer, but has a lower catalytic potential than SPCE. Meanwhile, the surface modification of the working electrode of flexible integrated three-electrode is very important to enhance the electrochemical sensing performance for SMZ.

Two-dimensional (2D) materials have attracted extensive research interest due to their unique physicochemical properties. Hexagonal boron nitride (h-BN) as an emerging 2D material, consisting of boron and nitrogen atoms aligned in a hexagonal structure via the strong covalent bonds and weak Van der Waals bilayer interaction. Overturning the initial reports that h-BN was non-conductive, researchers began applying 2D h-BN to the field of electrochemistry, particularly in electrochemical sensing fields [28,29]. It plays a prominent role in promoting the development of electrochemical sensors due to its large surface area, remarkable electron transport capabilities, and rich chemical stability [30,31].

Inspired by these aspects, we demonstrated a novel wireless electrochemical

sensor based on the home-made flexible integrated three-electrode for portable and fast detection of SAs, including SMZ, sulfanilamide (SN), sulfisoxazole (SIZ), sulfamethazine (SM2) and sulfapyridine (SPY). SMZ as one of the SAs carcinogens was used as the model analyte to optimize experimental conditions, and study the surface morphology and performance (electrochemical oxidation potential, electrochemical behaviors, cycle stability, electrochemically effective surface areas, repeatability, reproducibility and selectivity) of the home-made flexible integrated three-electrode. The flexible integrated three-electrode coupled with a portable mini electrochemical workstation was successfully applied for the determination of SMZ in milk and lake water. Finally, it was proved suitable for the detection of four SAs including SN, SIZ, SM2, SPY.

2. Experimental section

2.1. Materials

SMZ, SN, SIZ, SM2, and SPY (power form, purity ≥ 99%) was purchased from Stanford Analytical Chemicals Inc., and its stock solution was prepared with methanol. Silver and silver chloride ink (Ag/AgCl ink, YTXD-50-20, fineness ≤ 20 μm) and special thinner was obtained from Suzhou Yituo Biosensor Technology Co., Ltd. Pristine h-BN nanoflake solution (purity > 99%, sheet diameter from 50 to 200 nm) was obtained from Nanomaterial Technology Co., Ltd (Jiangsu, China). Commercial-available polyimide (PI) film (Kapton tape, thickness: 80 μm), a polymer sheet was used to fabricate the flexible integrated three-electrode composing of LIPG, was purchased from DuPont Company, America. 0.04 $mol \cdot L^{-1}$ (0.04 M) Britton-

Robinson (BR) buffer solution was used as supporting electrolyte and prepared with mixing stock solution of phosphoric acid, acetic acid, and boric acid. The various pH of the BR buffer was regulated by 0.01 M NaOH. All other reagents were analytical grade and no further purification unless otherwise stated. Deionized water (DI water, 18.2 MΩ · cm) was obtained from a Milli-Q water purification system and used in all experiments.

2.2. Instruments

The laser-induced process was carried out under ambient conditions using a home-made computer-controlled laser-scribing micromachining system (Nano Pro-III, Tianjin Jiayin Nanotechnology Co., Ltd., China, wavelength = 450 nm, precision = 10 μm, maximum power = 5.2 W, output laser beam < 10 μm, carving speed = 0.5 cm s^{-1}). A LIPG integrated three-electrode system consisting a partially unmodified LIPG served as a counter electrode, Ag/AgCl ink was casted on the porous graphene conductive track as the reference electrode, the three-electrode where the working electrode part was not modified was named $LIPG_0$, and it was named h-BN/$LIPG_0$ after being modified with h-BN. Portable mini electrochemical workstation with the PS Trace program was obtained from Red Matrix China Limited (PalmSens, Netherlands). The size of the portable mini electrochemical workstation is 10.0 × 6.0 × 3.4 cm, weight is 250 g, battery is PS3BATT. A traditional electrochemical workstation was obtained from Shanghai Chenhua Instrument Co., Ltd (CHI 620E, China). Chromatographic analysis was implemented by high performance liquid chromatography (HPLC) analyzer (Waters E2695, USA). SPSS (22.0) Statistical

142 Analysis Software was used to compare the obtained results using the proposed
143 electrochemical sensing method and HPLC.

144 2.3. Synthesis of LIPG electrodes

145 Before the preparation process, a home-made computer-controlled laser scribing
146 machine (wavelength = 450 nm, precision = 10 μm, maximum power = 5.2 W, output
147 laser beam < 10 μm, carving speed = 0.5 cm s^{-1}) was preheated for 30 min. To reduce
148 cost and incorporation functionality, PI film was applied as a flexible, reliable
149 platform for a PI film substrate was tailored into proper size, and cleaned by DI water,
150 ethanol and DI water for several times, and was fixed on a glass plate to avoid shape
151 deformation [19]. Then, a batch of original LIPGs was prepared under ambient
152 conditions according to a designed drawing (Fig. S2A), and individual electrodes
153 were carefully cut off with scissors. Finally, reference electrode was modified with
154 Ag/AgCl ink to obtain a complete and $LIPG_0$. A piece of PI film was pasted on the
155 long conducting part to isolate the working area and only the working area was in
156 contact with the electrolyte solution.

157 $LIPG_0$ without reference electrode part was obtained according to the above
158 steps, which was labeled as $LIPG_1$. $LIPG_1$ and saturated calomel electrode (SCE, as
159 the reference electrode) was used to form a three-electrode system. Working
160 electrode was modified with h-BN, and dried under infrared light to obtain h-
161 BN/$LIPG_0$ flexible integrated three-electrode.

162 2.4. Electrochemical measurements

163 The quantification of SMZ was operated in 5 mL 0.04 mol·L^{-1} (0.04 M) BR

buffer (pH = 5.0) by h-BN/LIPG$_0$ flexible integrated three-electrode, which was perfectly plugged into the portable mini electrochemical workstation interface and connect wirelessly to a smartphone via Bluetooth. The voltammetric analysis of SMZ and the optimization of experimental parameters were by differential pulse voltammetry (DPV) with the potential range of 0.2 - 1.2 V, the step potential of 0.004 V, the pulse potential of 0.05 V, the pulse width of 0.02 s. In 5 mM $K_3[Fe(CN)_6]$ and $K_4[Fe(CN)_6]$ containing 0.1 M KCl solution, the electrochemical behaviors and electro-oxidation mechanism with changeable scanning rate were performed by cyclic voltammetry (CV) with the step potential of 0.01 V. To contrast their performance potential, LIPG flexible integrated three-electrode was tested using a portable mini electrochemical workstation with a smartphone in comparison with traditional an electrochemical workstation with a desktop computer combined with both SCE and LIPG$_1$.

2.5. Real sample preparation

Lake water (collected from Jiangxi Agricultural University) was filtered using a 0.22 μm filter to remove the suspended particles. The filtered water sample was diluted with BR buffer (pH = 5.0). Commercial milk was acquired in a local market and was treated according to the following procedure: 40 mL of BR buffer/ACN 50% (v/v) was added to 5 g of milk and sonicated for 30 min. The mixture was then centrifuged at 4000 rpm for 15 min and filtered through a 0.22 μm filter. The filtrate was diluted with BR (pH = 5.0) to 50 mL to obtain the samples. To verify SMZ in real samples, recoveries of spiked samples were detected using the proposed method and

HPLC method.

2.6. Method validation

The assessment of validation parameters included linearity, LOD, and limit of quantification (LOQ), recovery and precision. The linearity was verified using buffer solution at ten concentration levels within the range of 0.50 – 362.5 μM for electrochemical sensor and the range of 0 - 39.5 μM for HPLC. We determined LOD and LOQ by repeating the blank test that can calculate the standard deviation (S_d) of blank test with signal to noise ratios (S/N) of 0.011 μM for LOD and 0.037 μM for LOQ. Recovery was determined by spiking two kinds of blank samples with the standard solution of SMZ at two levels: 27.5 μM and 55.0 μM. Precisions of the two methods were assessed by repeatability experiments in three replicates and expressed as the relative standard deviations (RSD).

3. Results and discussion

3.1 Preparation of flexible integrated electrode

One-step laser scribing on commercial PI films in air to form 3D porous graphene layers and then Ag/AgCl ink was drop-coated to a specific part to obtained individual $LIPG_0$ electrodes (Scheme 1). Firstly, a series of electrodes on PI sheet were fabricated by the laser scribing technique, and then the individual electrode was obtained by carefully cutting off with scissors. Secondly, the electrode area in contact with the solution is selectively passivated by a piece of PI film, where the diameter of working electrode was 3 mm. Finally, the flexible and integrated three-electrode ($LIPG_0$) was obtained. A comparison of $LIPG_0$ electrode with a paper clip was shown

in Fig. S2B, indicating the prepared $LIPG_0$ electrode was very pocket and portable.

The $LIPG_0$ electrode (drop-coated Ag/AgCl ink as reference electrode) was electrochemically modified in a specific part with h-BN to obtain the flexible integrated h-BN/$LIPG_0$ electrode. The flexible integrated electrode of h-BN/$LIPG_0$ was fit into a mini portable workstation and connects to the smartphone through Bluetooth to build a wireless sensor. The inset SEM image and voltammetry of 50 cycles presented the 3D porous surface and the stability of the $LIPG_0$ electrode. The electrochemical catalytic mechanism and rapid analysis of SMZ on the h-BN/$LIPG_0$ electrode were shown in Scheme 1. Finally, the on-site detection of raw lake water with the flexible portable sensor was performed.

The surface morphologies of the prepared $LIPG_0$ electrode and h-BN/$LIPG_0$ electrode were characterized by SEM (scanning electron microscope), TEM (transmission electron microscope) and HAADF-STEM (high-angle annular dark-field-scanning transmission electron microscopy). The top-view SEM images of $LIPG_0$ electrode (Fig. 1A&B) and h-BN/$LIPG_0$ electrode (Fig. 1G&H) showed characteristic graphene fringes and an ordered-porous flake foam-like structure. As this laser scribing was performed in air, the local availability of oxygen and moisture could burn-off some of the carbon during the graphitization to release CO and CO_2 gases, resulting in the porosity [32]. The cross-sectional SEM images revealed that both $LIPG_0$ electrode (Fig. 1C&D) and h-BN/$LIPG_0$ electrode (Fig. 1I&J) had more porous structure in different sizes, but it seemed that the h-BN/$LIPG_0$ electrode had a more regular perforated structure and thicker section than $LIPG_0$ electrode. These

porous and thicker sections enabled h-BN/LIPG$_0$ electrode to have a large active area and facilitate electrolyte penetration into three-dimensional active materials.

The microstructures of both LIPG$_0$ and h-BN/LIPG$_0$ electrode were investigated by TEM. It can be seen that the LIPG$_0$ (Fig. 1E&F) and the h-BN/LIPG$_0$ (Fig. 1K&L) had ripple-like wrinkled structure with few-layer features, in which the h-BN/LIPG$_0$ was more uniform and distinct than the LIPG$_0$ electrode. According to the report of Lin [33], the ripples were exposed edges of graphene layers in high-resolution TEM image, and the formation of these ripples could be attributed to thermal expansion caused by laser irradiation. To further determine the dispersion of elements, HAADF-STEM and the corresponding energy dispersive X-ray (EDX) elemental mapping of C, O, B and N elements of the h-BN/LIPG$_0$ electrode were carried out. The corresponding result was presented in Fig. 1M-P, showing that the uniform distribution of C, O, B and N elements in the h-BN/porous graphene. SEM-EDS (scanning electron microscope/energy dispersive X-ray spectrometer) image (Fig. 2A) revealed that the element composition and content of the h-BN/LIPG$_0$ electrode. The h-BN/LIPG$_0$ electrode contained C, O, B, N. Zhu [22] has reported the laser direct writing electrode only contained C and O elements, PI film contained N element, so the existent of B elements was originated from h-BN.

3.2 Performance of flexible integrated electrode

A LIPG flexible integrated three-electrode consists of an unmodified LIPG served as counter electrode, drop-coated Ag/AgCl ink on bare LIPG as reference electrode, h-BN/LIPG$_0$ as working electrode, and it perfectly plugged into the

portable mini-workstation interface, benefiting from its portability, pocket size and good conductive track. The portable mini-workstation connects wirelessly to a smartphone via Bluetooth, and the voltammetric analysis was test by the PSTrace program.

To study the electrocatalytic potential of the self-made LIPG flexible integrated three-electrode to SMZ, four three-electrode systems and two different sensing devices were established, respectively (Fig. S3). The electrode of $LIPG_0$ and h-$BN/LIPG_0$ (both Ag/AgCl ink was drop-coated as the reference electrode) coupled with portable mini-workstation. The electrode of $LIPG_1$ and h-$BN/LIPG_1$ (both SCE served as the reference electrode) coupled with traditional workstation were used to detect the same concentration of SMZ. The result of the electrocatalytic potential comparison was shown in Fig. 2B. It presented that the electrocatalytic potential of $LIPG_0$ (0.59 V) and h-$BN/LIPG_0$ electrode (0.56 V) on portable mini-workstation both lower than $LIPG_1$ (0.76 V) and h-$BN/LIPG_1$ electrode (0.76 V) on conventional electrochemical workstation, the peak current of $LIPG_0$ electrode (4.1 μA) and h-$BN/LIPG_0$ electrode (8.6 μA) was higher than those of $LIPG_1$ (2.1 μA) electrode and h-$BN/LIPG_1$ (2.8 μA) electrode, respectively. Therefore, with the same working electrode, the detection effect is better on the portable workstation using flexible integrated three-electrode than on the traditional non-integrated rigid electrode and workstation. Surprisingly, the response time of portable mini-workstation using DPV method was ten times (only about 6 seconds) faster than conventional electrochemical workstation (at least 60 seconds), this is a valuable feature for on-site rapid detection

in comparison [23].

The current response and electrocatalytic potential of commercial SPCE to SMZ of the same concentration on portable mini-workstation were also compared, and the sensing devices and the results were shown in the Fig. S4A and Fig. S4B, respectively. The current response of $LIPG_0$ electrode (4.1 μA) and h-BN/$LIPG_0$ (8.6 μA) electrode was larger than that of SPCE (1.3 μA) and h-BN/SPCE (3.2 μA), the electrocatalytic potential of $LIPG_0$ (0.59 V) and h-BN/$LIPG_0$ (0.56 V) was lower than SPCE (0.60 V) and h-BN/SPCE (0.66 V). Therefore, the home-made flexible integrated electrode of h-BN/$LIPG_0$ had a favorable advantage in lower electrocatalytic potential, high current response and rapid detection for SMZ.

The electrochemical behaviors of ferrous/ferricyanide on h-BN/$LIPG_0$ and $LIPG_0$ electrodes were investigated by CV in 5 mM $K_3[Fe(CN)_6]$ and $K_4[Fe(CN)_6]$ containing 0.1 M KCl from the potential range of -0.2 V - 1.2 V at a scan rate of 50 mV s^{-1} (Fig. 2C), showing that the potential difference between the oxidation peak and reduction peak at the h-BN/$LIPG_0$ electrode was significantly smaller than that of $LIPG_0$ electrode. It showed that the electrocatalytic oxidation capacity of the $LIPG_0$ electrode modified by h-BN was stronger than that of the $LIPG_0$ electrode.

The cycle stability of the h-BN/$LIPG_0$ electrode with continuous CVs scans of 50 cycles has unchanged (Fig. 2D). The RSD values of the h-BN/$LIPG_0$ electrode with both anode and cathode peak currents were 2.79% and 2.94%, respectively, showing that the h-BN/$LIPG_0$ electrode had better electrochemical cycle stability and electrode stability.

Electrochemically effective surface areas (A) of the h-BN/LIPG$_0$ electrode was determined by chronocoulometry using 5 mM $K_3[Fe(CN)_6]$ containing 0.1 M KCl as supporting electrolyte (Fig. 2E). According to equation (1) of Anson:

$$Q(t) = 2nFACD^{1/2}t^{1/2}\pi^{-1/2} + Q_{dl} + Q_{ads} \qquad \text{Equation. (1)}$$

where n is the electron number (n = 1), D is the diffusion coefficient involved in the electrochemical reaction of $[Fe(CN)_6]^{3-}$ solution (D = 7.6 × 10^{-6} cm^2 s^{-1}), C is the substrate concentration, and other symbols have their usual meaning. According to the linear relationships of Q - $t^{1/2}$ as shown in Fig. 2F, the effective surface area was calculated as 0.201 cm^2, 1.198 cm^2 for the LIPG$_0$ and h-BN/LIPG$_0$, respectively. The result revealed that the A of the h-BN/LIPG$_0$ electrode was 5.96 times greater than the LIPG$_0$ electrode and substantially enlarging the electrochemical active sites.

3.3 Optimization of sensing parameters

The modified volume of the h-BN nanoflake solution can affect the electrochemical signal of the sensor for SMZ. If the modified volume is too little, the surface of electrode cannot be completely covered and the advantages of modified materials cannot be fully played. Conversely, the sufficient amounts of modified materials are more favorable for electron transfer. Therefore, it is necessary to optimize the amount of electrode modified material. As shown in Fig. 3A, the current response reached the maximum when the modified volume was 0.6 μL, indicating the electron transfer performance of the sensor was the best. Therefore, 0.6 μL h-BN nanoflake solution was modified on LIPG$_0$ electrode for subsequent experiments.

The CVs corresponding to various scan rates (v) of 50 μM SMZ on the h-

318 BN/LIPG$_0$ electrode were investigated in BR of pH 5.0. As shown in Fig. 3B with the
319 increase of scan rates from 20 mV s^{-1} to 100 mV s^{-1}, it was observed that the
320 oxidation peak potentials significantly shifted towards a more positive potential. The
321 curves of the I_{pa} increased linearly with the square root of scan rates ($v^{1/2}$, R^2 =
322 0.9941, Fig. 3D) and the logarithm of scan rate (ln v, R^2 = 0.9941, Fig. 3E), but the
323 curve showed a bending characteristic with the scan rates (v, Fig. 3C), revealing that
324 the reaction of SMZ could be a typically irreversible diffusion control process. The
325 linear relationship between E_{pa} and ln v for SMZ could be expressed as E_{pa} = 0.9257 +
326 0.0665 ln v (R^2 = 0.9929) (Fig. 3E), and E_{pa} could be calculated according to the
327 equation (2) of Laviron theory.

328 $$E_{pa} = E^0 + \left(\frac{RT}{anF}\right) \ln\left(\frac{RTk^0}{anF}\right) + \left(\frac{RT}{anF}\right) \ln v \qquad \text{Equation. (2)}$$

329 Where α is the transfer coefficient, k^0 is the rate constant of the reaction, v is the
330 scan rate, n is the electron-transfer number; E^0 is the formal standard potential, R, T,
331 and F have their usual meanings (R = 8.314 J mol^{-1} K^{-1}, T = 298 K, and F = 96,485 C
332 mol^{-1}). In general, the value of α is between 0.3 and 0.7 [34], therefore n is calculated
333 to be 1 from the slope of the linear regression equation, which was in lined with
334 previously reported results [35].

335 The electrochemical reaction involves proton-transfer reaction and it is
336 influenced by the pH of the electrolyte. The effect of pH on the electrocatalytic
337 oxidation of SMZ on h-BN/LIPG$_0$ was studied by DPV in 0.04 M BR with pH range
338 of 3.0 ~ 9.0 (Fig. 3F). There were obvious differences in peak currents (I_{pa}) and
339 potentials (E_{pa}) to SMZ under different pH conditions. The maximum peak current

was found at pH value of 5.0. In addition, the linear relationship between E_{pa} and pH for SMZ (Fig. 4A) could be expressed as E_{pa} = 0.940 - 0.045 pH (R^2 = 0.9947). The number of proton (m) participating in the electrochemical reaction was calculated according to Nernst equation (2).

$$E_{pa} = E^0 + \left(\frac{RT}{nF}\right)\ln\left(\frac{[Ox]}{[Red]}\right) + \left(\frac{2.303mRT}{nF}\right)pH \qquad \text{Equation. (2)}$$

Where m is the number of protons in the electrochemical reaction and it could be further calculated by the slope of the linear regression equation. Thus, m was calculated to be 1 for SMZ, it was in agreement with the mechanism of the previous report [36]. The electrocatalytic oxidation mechanism of SMZ on h-BN/LIPG$_0$ as shown in Scheme S1.

3.4 The fabricated wireless sensor for detecting SMZ

The determination of SMZ using DPV at h-BN/LIPG$_0$ electrode was performed in BR (pH = 5.0). Scan the blank buffer solution at least 6 times before each test to stabilize the background current and ensures reproducibility of the electrode in the voltammetry measurements. The peak current of SMZ increased with its concentration (Fig. 4B), and there is a linear relationship between anodic peak current and SMZ concentration in the range from 0.5 to 362.5 μM, its linear equation was I_{pa} = 3.5098 C + 0.2154 (R^2 = 0.9963, Fig. 4C). The LOD was 0.011 μM (LOD = 3 σ/m, where σ is the standard deviation of 20 times electrochemical responses for the blank solution and m is the slope of the calibration plot) and the LOQ was 0.037 μM. In comparison with previous reported results (Table S1), it could be observed that the fabricated h-BN/LIPG$_0$ sensor was not only easy to use, but had a low electrochemical

362 oxidation potential, a low LOD, and widespread linear ranges for SMZ. These results
363 indicated that the h-BN/LIPG$_0$ electrode was an excellent electrochemical sensing
364 electrode for the detection of SMZ.

365 3.5 Repeatability, reproducibility and selectivity

366 The repeatability of the h-BN/LIPG$_0$ electrode for the voltammetric response of
367 50 μM SMZ was estimated using the same modified by 20th successive
368 measurements under the optimum conditions. As shown in Fig. 4D, the RSD value of
369 the repeatable peak currents was 4.01%, showing a good repeatability of the proposed
370 sensor. The reproducibility of the prepared ten h-BN/LIPG$_0$ electrodes was evaluated
371 for the determination of SMZ under the same conditions, respectively, the RSD value
372 was 4.65% (Fig. 4E), indicating that the sensor had good reproducibility. In order to
373 investigate the effect of bending on the performance of the h-BN/LIPG$_0$ electrode, the
374 current response before and after bending 50 times were studied, and the result
375 showed that the current was almost the same before and after bending.

376 The selectivity for the voltammetric detection of SMZ at the h-BN/LIPG$_0$
377 electrode was investigated and indicated in Fig. 4F. Firstly, 50 μM SMZ was added
378 and detected in 0.04 M BR (pH = 5.0), then, the possible interferents such as NaCl,
379 KCl, $MgCl_2$, $CaCl_2$ with 100-fold concentration, glucose with 10-fold concentration
380 of SMZ were added successively and tested in the presence of 50 μM SMZ. Glutamic
381 acid, arginine and hypoxanthine with 1-fold concentration of SMZ were also tested.
382 The results in Fig. 4F indicated that the determination of SMZ not influenced (RSD
383 value < 5%) by the possible interfering substances, hence, the obtained sensors had a

good anti-interferent ability for SMZ.

In the previous voltammetry sensors, many studies only focused on the detection of single sulfonamide, but few studies analyzed the effect of sulfonamide analogs to the current response of SMZ [36-40]. In this work, we tested the influence of current repose in the presence of the equal amount of SN and SM2, the change value of SMZ current response was 10.3% and 10.9%, respectively. It is possible that the sulfonamide analogues have very similar oxidation potentials, so the simultaneous detection of multi-sulfa antibiotics by voltammetric methods still presents high mutual interference [41].

3.6 Practical application of portable sensor

The feasibility and applicability of the proposed h-BN/LIPG$_0$ sensor for the detection of SMZ were performed by the portable sensor based on a smartphone and a reference HPLC method (national standard method of China) in lake water and milk (Table 1). The RSD values were less than 5% and recoveries of the samples were in the range of 97.5 – 108.2% of the two methods, indicating that the proposed method had a satisfactory precision and feasibility. Moreover, the results of the proposed portable sensor and the HPLC method were compared by the paired t-test with SPSS (22.0) Statistical Analysis Software (Table S2). Results of analysis showed there was no significant difference between the two methods, which also suggesting a promising practical application in spiked sample analyses of the portable sensor.

The proposed method was used to detection other four SAs (SN, SIZ, SM2, SPY) with linear concentration range of 2.08 μM to 233.33 μM. The voltammogram

and corresponding linear relationships were demonstrated in Fig. 5. It indicated that the electrochemical oxidation potential of four SAs were similar with SMZ and there was a good linear relationship between concentrations and current responses on the h-BN/LIPG$_0$ electrode, the R^2 values were 0.9887, 0.9871, 0.9955 and 0.9868, respectively. This may be due to the fact that all five SAs have the structure of benzenesulfonamide, so the catalytic potential is very close, which was consistent with the previous interference experiment. However, in the rational use of drugs, generally only one sulfonamide is used to prevent or treat mild infection. So, through the linear equations of five SAs, it can be seen that the proposed portable, fast sensing method had a good effect in detecting these five SAs, respectively.

4. Conclusion

A home-made flexible integrated three-electrode fabricated by laser writing technology as a low-cost, portable and fast sensing platform was successfully developed for electrochemical detection of SAs. The novel flexible integrated three-electrode has the characteristics of easy-to-prepare, low cost, 3D porous interconnected network, larger effective surface area, high stability, good selectivity, low oxidation potential and satisfactory recoveries to SMZ. It has been confirmed that the proposed method has no difference with HPLC method and can be used for the detection of five SAs. Such miniaturized integrated electrode could allow testing for SAs to more reliable, easier and inexpensive, and has enormous potential in outdoor analysis.

Acknowledgments

This work is supported by the Key of Natural Science Foundation of Jiangxi Province (20192ACB20007), National Natural Science Foundation of China (51962007).

References

[1] S. Fekadu, E. Alemayehu, R. Dewil, & B.V.D. Bruggen, Pharmaceuticals in freshwater aquatic environments: A comparison of the African and European challenge, Sci. Total Environ. 9 (2018) 324-337. https://doi.org/ 10.1016/j.scitotenv.2018.11.072.

[2] L. Liu, Q. Wan, X. Xu, S. Duan, & C. Yang, Combination of micelle collapse and field-amplified sample stacking in capillary electrophoresis for determination of trimethoprim and sulfamethoxazole in animal-originated foodstuffs, Food Chem. 219 (2017) 7–12. https://doi.org/10.1016/j. foodchem

[3] W. Xue, F. Li, Q. Zhou, Degradation mechanisms of sulfamethoxazole and its induction of bacterial community changes and antibiotic resistance genes in a microbial fuel cell, Bioresour. Technol. 289 (2019) 121632-121640. https://doi.org/10.1016/j.biortech.2019.121632.

[4] Y. Ou, L. Yao, Y. Li, C. Bai, G. Peng, Magnetically separable Fe-MIL-88B_NH_2 carbonaceous nanocomposites for efficient removal of sulfamethoxazole from aqueous solutions, J. Colloid Interface Sci. 570 (2020) 163-172. https://doi.org/10.1016/j.jcis.2020.02.116.

[5] D. Fatta-Kassinos, S. Meric, A. Nikolaou, Pharmaceutical residues in environmental waters and wastewater: current state of knowledge and future research, Anal. Bioanal. Chem. 399 (2010) 251-275.

452 https://doi.org/10.1007/s00216-010-4300-9.

453 [6] X.T. Xie, S.Y. Huang, J. Zhen, & G.F. Ouyang, Trends in sensitive detection and
454 rapid removal of sulfonamides: A review, J. Sep. Sci. 43 (2020) 1634–1652.
455 https://doi.org/10.1002/jssc.201901341.

456 [7] L.A. Li, Y. Zhu, F.Y. Zhang, H. Li, J.I. Iqbal, T. Wu, Y.P. Du, Rapid detection of
457 sulfamethoxazole in plasma and food samples with in-syringe membrane SPE
458 coupled with solid-phase fluorescence spectrometry, Food Chem. 320 (2020a) 1–
459 26. https://doi.org/10.1016/j.foodchem.2020.126612.

460 [8] T. Li, C. Wang, Z. Xu, & A. Chakraborty, A coupled method of on-line solid
461 phase extraction with the UHPLCMS/MS for detection of sulfonamides
462 antibiotics residues in aquaculture, Chemosphere. 254 (2020b) 126765-126773.
463 https://doi.org/10.1016/j.chemosphere.2020.126765.

464 [9] Y. Ge, P. Liu, L.J. Xu, M.S. Qu, W.X. Hao, H. Liang, Y.Y. Sheng, Y.F. Zhu, Y.P.
465 Wen, A portable wireless intelligent electrochemical sensor based on layer-by-
466 layer sandwiched nanohybrid for terbutaline in meat products, Food Chem. 371
467 (2022) 1331140-1331148. https://doi.org/10.1016/j.foodchem.2021.131140.

468 [10] Y.F. Zeng, M.B. Camarada, X.Y. Lu, K.J. Tang, W.Q. Li, D.Y. Qiu, Y.P. Wen,
469 G.P. Wu, Q.S. Luo, L. Bai, Detection and electrocatalytic mechanism of
470 zearalenone using nanohybrid sensor based on copper-based metal-organic
471 framework/magnetic Fe_3O_4-graphene oxide modified electrode, Food Chem. 370
472 (2022) 131024-131034. https://doi.org/10.1016/j.foodchem.2021.131024.

473 [11] Z. Guo, & L. Gang, A Portable Electrochemical System for the On-Site
474 Detection of Heavy Metals in Farmland Soil Based on Electrochemical Sensors,

IEEE. Sens. J. 18 (2018) 5645-5655. https://doi.org/10.1109/JSEN.2018.2845306.

[12] Y.Y. Sheng, W.B. Qian, J.P. Huang, B.L. Wu, J. Yang, T. Xue, Y. Ge, Y.P. Wen, Electrochemical detection combined with machine learning for intelligent sensing of maleic hydrazide by using carboxylated PEDOT modified with copper nanoparticles, Microchim. Acta. 186 (2019) 1–12. https://doi.org/10.1007/s00604-019-3652-x.

[13] Y.C. Zhao, J.Z. Xiang, H. Cheng, X.J. Liu, F. Li, Flexible photoelectrochemical biosensor for ultrasensitive microRNA detection based on concatenated multiplex signal amplification, Biosens. Bioelectron. 194 (2021) 113581-113589. https://doi.org/10.1016/j.bios.2021.113581.

[14] J. Wang, Portable electrochemical systems, TrAC, Trends Anal. Chem. 21(2002) 226-232. https://doi.org/10.1016/S0165-9936(02)00402-8.

[15] F. Conzuelo, M. Gamella, S. Campuzano, D.G. Pinacho, J.M. Pingarrón Disposable and integrated amperometric immunosensor for direct determination of sulfonamide antibiotics in milk, Biosens. Bioelectron. 36 (2012) 81-88. https://doi.org/10.1016/j.bios.2012.03.044.

[16] W. Zhang, R.G. Wang, F. Luo, P. L. Wang, Z.Y. Lin, Miniaturized electrochemical sensors and their point-of-care applications, Chin. Chem. Lett. 31 (2020) 589-600. https://doi.org/10.1016/j.cclet.2019.09.022.

[17] X.J Liu, H. Cheng, Y.C. Zhao, Y. Wang, F. Li, Portable electrochemical biosensor based on laser-induced graphene and MnO_2 switch-bridged DNA

signal amplification for sensitive detection of pesticide, Biosens. Bioelectron. 199 (2022) 113906- 113914. https://doi.org/10.1016/j.bios.2021.113906.

[18] X.J. Liu, X. Gao, L.M. Yang, Y.C. Zhao, F. Li, Metal–organic framework-functionalized paper-based electrochemical biosensor for ultrasensitive exosome assay, Anal. Chem. 93 (2021) 11792-11799. https://doi.org/10.1021/acs.analchem.1c02286.

[19] X.Y. Zhu, L. Lin, R.M. Wu, Y.F. Zhu, Y.Y. Sheng, P.C. Nie, P. Liu, Y.P. Wen, Portable wireless intelligent sensing of ultra-trace phytoregulator α-naphthalene acetic acid using self-assembled phosphorene/Ti_3C_2-MXene nanohybrid with high ambient stability on laser induced porous graphene as nanozyme flexible electrode, Biosens. Bioelectron. 179 (2021) 113062-11307. https://doi.org/10.1016/j.bios.2021.113062.

[20] M.H. Li, P.C. Zhou, X.Q. Wang, Y.P. Wen, L.L. Xu, J. Q. Hu, Z. Huang, M.F. Li, Development of a simple disposable laser-induced porous graphene flexible electrode for portable wireless intelligent votammetric nanosensing of salicylic acid in agro-products, Comput. Electron. Agr. 191 (2021) 106502-106511. https://doi.org/10.1016/j.compag.2021.106502.

[21] L.L. Xu, R.M. Wu, X.Y. Zhu, X.Q. Wang, X. Geng, Y. Xiong, T. Chen, Y.P. Wen, S.R. Ai, Intelligent analysis of maleic hydrazide using a simple electrochemical sensor coupled with machine learning, Anal. Methods. 13 (2021) 4662-4673. https://doi.org/10.1039/D1AY01261D.

[22] Y.F. Zhu, P. Liu, T. Xue, J.K. Xu, & Y.P. Wen, Facile and rapid one-step mass production of flexible 3d porous graphene nanozyme electrode via direct laser-

writing for intelligent evaluation of fish freshness, Microchem. J. 162 (2020) 105855-105865. https://doi.org/10.1016/j.microc.2020.105855.

[23] D.Y. Qiu, X.Q. Wang, Y.P. Wen, Y.F. Zeng, W.Q. Li, L. Zhao, L.L. Chen, J.H. Xiong, K.J. Tang, A low-cost wireless intelligent portable sensor based on disposable laser-induced porous graphene flexible electrode decorated by gold nanoshells for rapid detection of sulfonamides in aquatic products, Food Anal. Methods, 8 (2022) 1-11. https://doi.org/10.1007/s12161-021-02198-8.

[24] F.D. Munteanu, A.M. Titoiu, J.L. Titoiu, A. Vasilescu, Detection of antibiotics and evaluation of antibacterial activity with screen-printed electrodes, Sensors. 18 (2018) 901-927. https://doi.org/10.3390/s18030901.

[25] A. Lahcen, A. Amine, Mini-review: recent advances in electrochemical determination of sulfonamides, Anal. Lett. 51 (2018) 424-441. https://doi.org/10.1080/00032719.2017.1295977.

[26] C. Chen, Y.C. Chen, Y.T. Hong, T.W. Lee, J.F. Huang, Facile fabrication of ascorbic acid reduced graphene oxide-modified electrodes toward electroanalytical determination of sulfamethoxazole in aqueous environments, Chem. Eng. J. 352 (2018) 188-197. https://doi.org/10.1016/j.cej.2018.06.110.

[27] L.F. Sgobbi, C.A. Razzino, S.A.S. Machado, A disposable electrochemical sensor for simultaneous detection of sulfamethoxazole and trimethoprim antibiotics in urine based on multiwalled nanotubes decorated with Prussian blue nanocubes modified screen-printed electrode, Electrochim. Acta. 191 (2016) 1010-1017. http://dx.doi.org/10.1016/j.electacta.2015.11.151.

[28] G.M. Ferrari, S.J. Rowley-Neale and C.E. Banks, Recent advances in 2D hexagonal boron nitride (2D h-BN) applied as the basis of electrochemical

sensing platforms, Anal. Bioanal. Chem. 13 (2020) 663-672. https://doi.org/10.1007/s00216-020-03068-8.

[29] S. Angizi, M. Khalaj, S.A.A. Alem, A. Pakdel, A. Simchi, Review-towards the two-dimensional hexagonal boron nitride (2D h-BN) electrochemical sensing platforms, J. Electrochem. Soc. 167 (2020) 126513-126532. https://doi.org/10.1149/1945-7111/abaf29.

[30] K. Zhang, Y. Feng, F. Wang, Z. Yang, J. Wang, Two dimensional hexagonal boron nitride (2D h-BN): synthesis, properties and applications, J. Mater. Chem. C. 5 (2017) 11992–12022. https://doi.org/10.1039/c7tc04300g.

[31] A.F. Khan, E.P. Randvii, D.A.C. Brownson, X.B. Ji, G.C. Smith, C.E. Banks, 2D hexagonal boron nitride (2D h-BN) explored for the electrochemical sensing of dopamine, Anal. Chem. 88 (2016) 9729–9737. https://doi.org/10.1021/acs.analchem.6b02638.

[32] P. Nayak, N. Kurra, C. Xia, H.N. Alshareef, Highly efficient laser scribed graphene electrodes for on-chip electrochemical sensing applications, Adv Electron. Mater. 2(2016) 1600185-1600196. https://doi.org/10.1002/aelm.201600185.

[33] J. Lin, Z.W. Peng, Y.Y. Liu, F. Ruiz-Zepeda, R. Ye, E.L.G. Samuel, M.J. Yacaman, B.I. Yakobson, & M. James, Laser-induced porous graphene films from commercial polymers, Nat. Commun. 5 (2014) 5714-5722. https://doi.org/10.1038/ncomms6714.

[34] E. Laviron, General expression of the linear potential sweep voltammogram in the case of diffusionless electrochemical systems, J. Electroanal. Chem. 101

(1979) 19-28. https://doi.org/10.1016/S0022-0728(79) 80075-3.

[35] A.E Radi, A. Eissa, T. Wahdan, Voltammetric behavior of mycotoxin zearalenone at single walled carbon nanotubes screen-printed electrode, Anal. Methods. 11 (2019) 4494-4500. https://doi.org/10.1039/C9AY01400D.

[36] S. Salmanpour, M.A. Khalilzadeh, H. Karimi-Maleh, D. Zareyeea, An electrochemical sensitive sensor for determining sulfamethoxazole using a modified electrode based on biosynthesized nio nanoparticles paste electrode, Int. J. Electrochem. Sci. 14 (2019) 9552-9561. https://doi.org/10.20964/2019.10.03.

[37] M. Shabani-Nooshabadi, and M. Roostaee, Modification of carbon paste electrode with NiO/graphene oxide nanocomposite and ionic liquids for fabrication of high sensitive voltammetric sensor on sulfamethoxazole analysis, J. Mol. Liq. 220 (2016) 329-333. https://doi.org/10.1016/j.molliq.2016.05.001.

[38] M. Meshki, M. Behpour, and S. Masoum, Application of Fe doped ZnO nanorods-based modified sensor for determination of sulfamethoxazole and sulfamethizole using chemometric methods in voltammetric studies, J. Electroanal. Chem. 740 (2015) 1-7. https://doi.org/10.1016/j.jelechem.2014.12.008.

[39] S. Tajik, H. Beitollahi, M.S. Asl, H.W. Jang, M. Shokouhimehrde, BN-Fe_3O_4-Pd nanocomposite modified carbon paste electrode: Efficient voltammetric sensor for sulfamethoxazole, Ceram. Int. 47 (2021) 13903-13911. https://doi.org/10.1016/j.ceramint.2021.01.257.

589 [40] Y. Abdollah, S. Azim, Silver-filled MWCNT nanocomposite as a sensing
590 element for voltammetric determination of sulfamethoxazole, Anal. Chim. Acta.
591 1039 (2018) 51-58. https://doi.org/10.1016/j.aca.2018.07.061.
592 [41] M. Arvand, R. Ansari, L. Heydari, Electrocatalytic oxidation and differential
593 pulse voltammetric determination of sulfamethoxazole using carbon nanotube
594 paste electrode, Mater. Sci. Eng. C. 31 (2011) 1819–1825.
595 https://doi.org/10.1016/j.msec.2011.08.014.

596 **Figure caption：**

597 **Fig. 1.** SEM (A, B), cross-sectional SEM (C, D), and TEM (E, F) of $LIPG_0$. SEM (G,
598 H), cross-sectional SEM (I, J) and TEM (K, L) of h-BN/$LIPG_0$. HAADF-STEM
599 image (inserted in M) of h-BN/$LIPG_0$ electrode and corresponding EDX-mapping
600 images mapping images of C element (M), O element (N), B element (O) and N
601 element (P).

602 **Fig. 2.** (A) EDS elemental analyses of h-BN/$LIPG_0$; (B) Comparison of peak
603 potentials to SMZ detected by h-BN modified LIPG electrodes using different
604 reference electrodes (Ag/AgCl ink or SCE); (C) Cyclic voltammetric behavior (scan
605 rate was 100 mV s^{-1}) of SMZ at $LIPG_0$ and h-BN/$LIPG_0$ electrodes in the same
606 concentration of SMZ; (D) Stability of with successive CVs scans of 50 cycles of h-
607 BN/$LIPG_0$ electrode; (E) The plots of Q - t curves of SMZ at $LIPG_0$ and h-BN/$LIPG_0$
608 electrodes; (F) The plots of Q - $t^{1/2}$ curves of SMZ at $LIPG_0$ and h-BN/$LIPG_0$
609 electrodes.

610 **Fig. 3.** (A) Optimization of modification amount of h-BN at h-BN/$LIPG_0$ electrode;

(B) CV curves of h-BN/LIPG$_0$ from 20 - 100 mV s^{-1}; Plots of v – I (C), $v^{1/2}$- I (D), ln$v$ – E (E) were presented; (F) DPV of 5 × 10^{-5} mol/L SMZ with different pH values at h-BN/LIPG$_0$ electrode.

Fig. 4. (A) The effect of different pH on oxidation peak potentials (straight line) and oxidation peak current values (curve) for SMZ in 0.04 M BR with scan rate 100 mV s^{-1}; (B) DPV of SMZ at h-BN/LIPG$_0$ electrode in 0.04 M BR containing concentration from 0.5 - 362.5 μM at h-BN/LIPG$_0$ electrode; (C) The linear equation of SMZ with different concentration from 0.5 - 36.25 μM; repeatability (D) and reproducibility (E) of h-BN/LIPG$_0$ electrode for the determination of 5 × 10^{-5} mol/L SMZ in BR (pH 5.0); (F) Adding SMZ (a), NaCl (b), KCl (c), $MgCl_2$ (d), $CaCl_2$ (e), glucose (f), glutamic acid (g), arginine (h) and hypoxanthine (i) in order in the same buffer to study the effect of possible interfering substances on SMZ detection.

Fig. 5 The proposed wireless and flexible electrochemical sensor based on smartphone for the detection of four SAs with linear concentration range of 2.08 μM to 233.33 μM and corresponding linear relationships: SN (A, B), SIZ (C, D), SM2 (E, F), SPY (G, H).

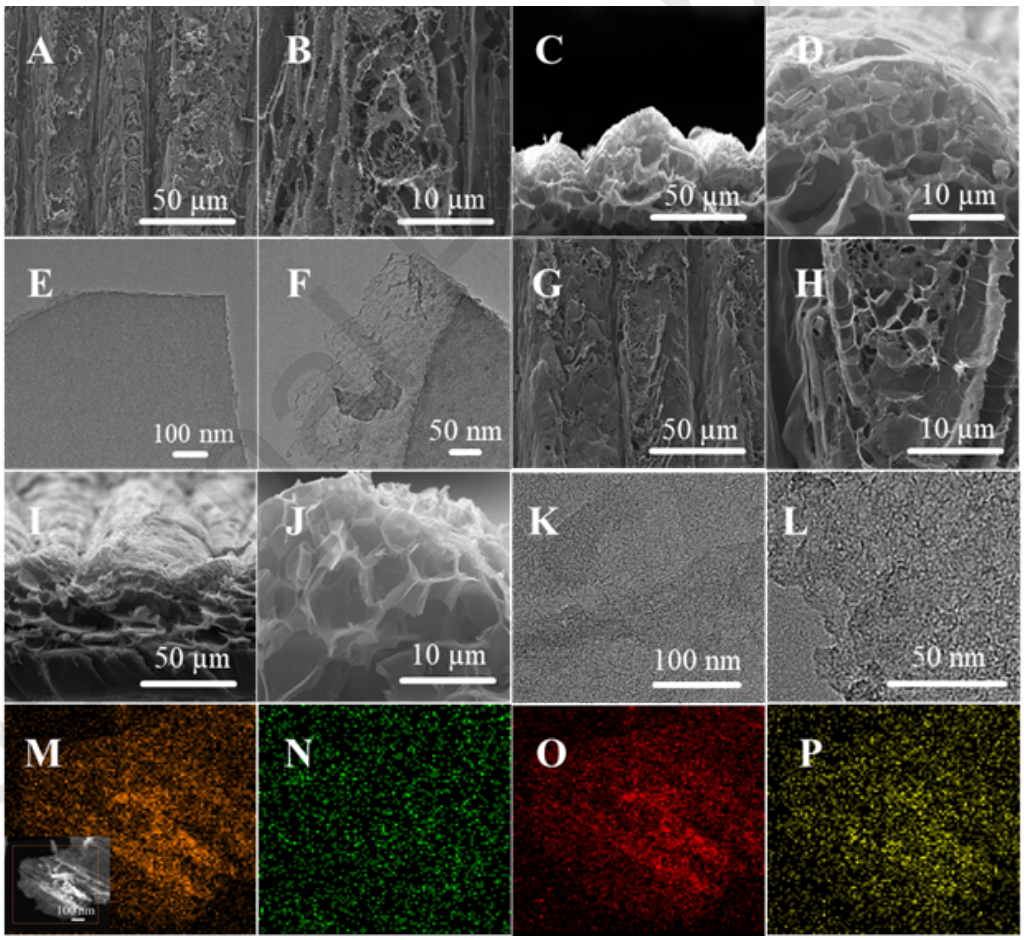

Fig. 1. SEM (A, B), cross-sectional SEM (C, D), and TEM (E, F) of $LIPG_0$. SEM (G, H), cross-sectional SEM (I, J) and TEM (K, L) of h-BN/$LIPG_0$. HAADF-STEM

650 image (inserted in M) of h-BN/LIPG$_0$ electrode and corresponding EDX-mapping
651 images mapping images of C element (M), O element (N), B element (O) and N
652 element (P).

653

654

655

656

657

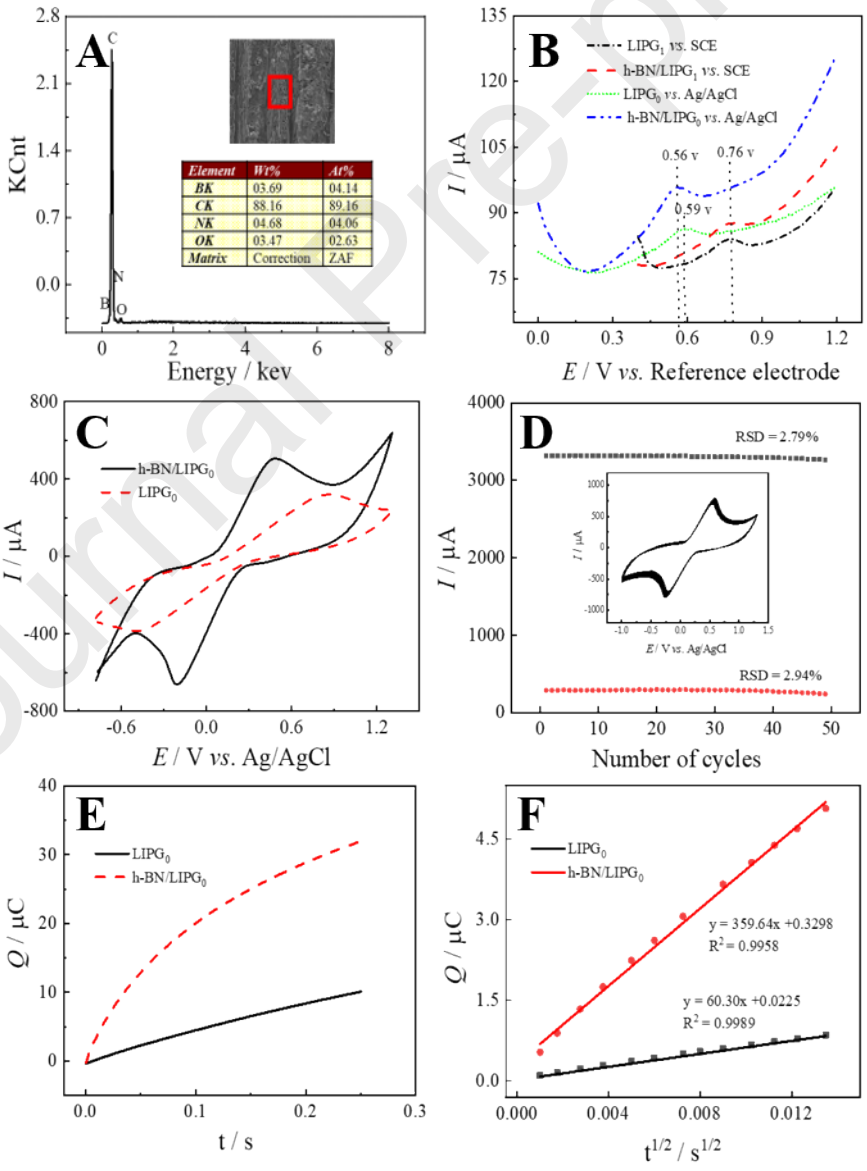

658

659 **Fig. 2.** (A) EDS elemental analyses of h-BN/LIPG$_0$; (B) Comparison of peak
660 potentials to SMZ detected by h-BN modified LIPG electrodes using different
661 reference electrodes (Ag/AgCl ink or SCE); (C) Cyclic voltammetric behavior (scan
662 rate was 100 mV s^{-1}) of SMZ at LIPG$_0$ and h-BN/LIPG$_0$ electrodes in the same
663 concentration of SMZ; (D) Stability of with successive CVs scans of 50 cycles of h-
664 BN/LIPG$_0$ electrode; (E) The plots of Q - t curves of SMZ at LIPG$_0$ and h-BN/LIPG$_0$
665 electrodes; (F) The plots of Q - $t^{1/2}$ curves of SMZ at LIPG$_0$ and h-BN/LIPG$_0$
666 electrodes.

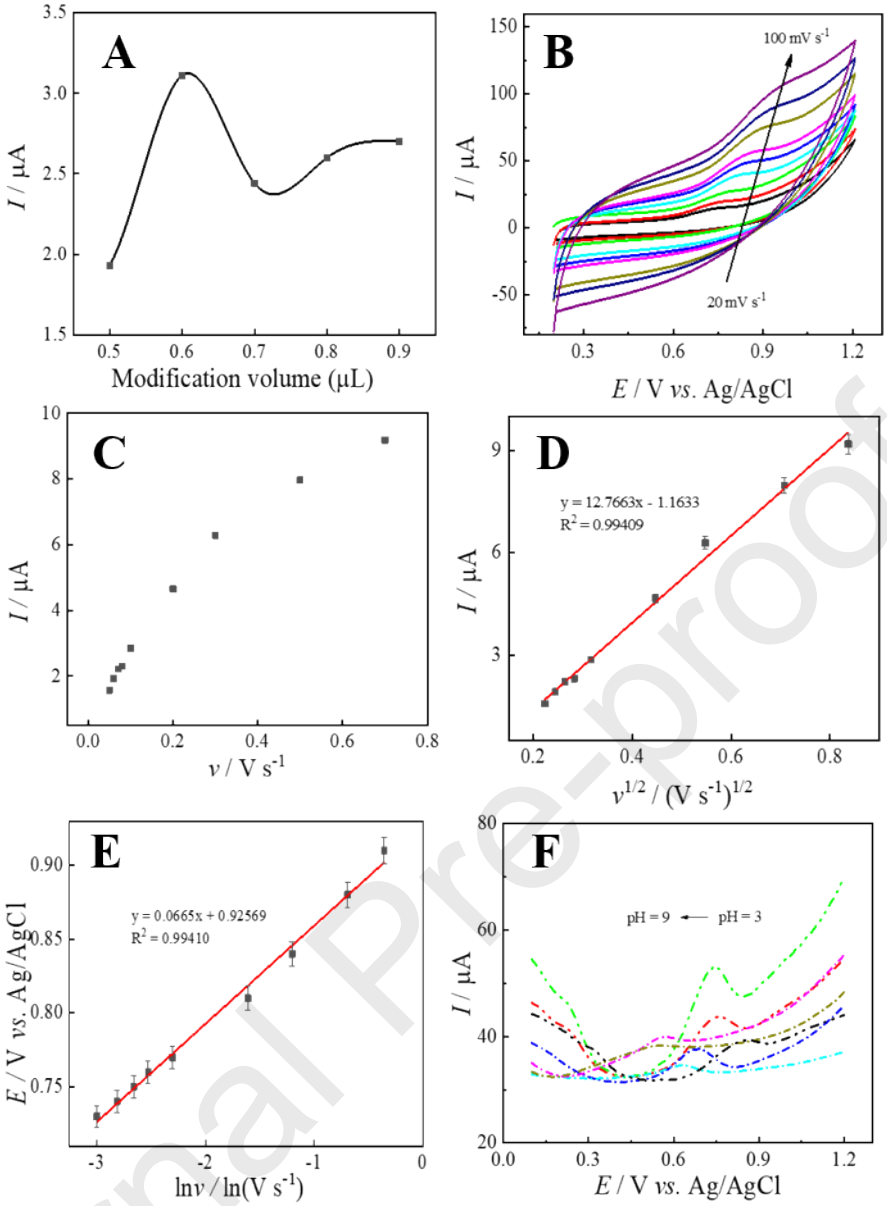

667

668 **Fig. 3.** (A) Optimization of modification amount of h-BN at h-BN/LIPG$_0$ electrode;

669 (B) CV curves of h-BN/LIPG$_0$ from 20 - 100 mV s^{-1}; Plots of v – I (C), $v^{1/2}$- I (D), ln$v$

670 – E (E) were presented; (F) DPV of 5 × 10^{-5} mol/L SMZ with different pH values at h-

671 BN/LIPG$_0$ electrode.

672

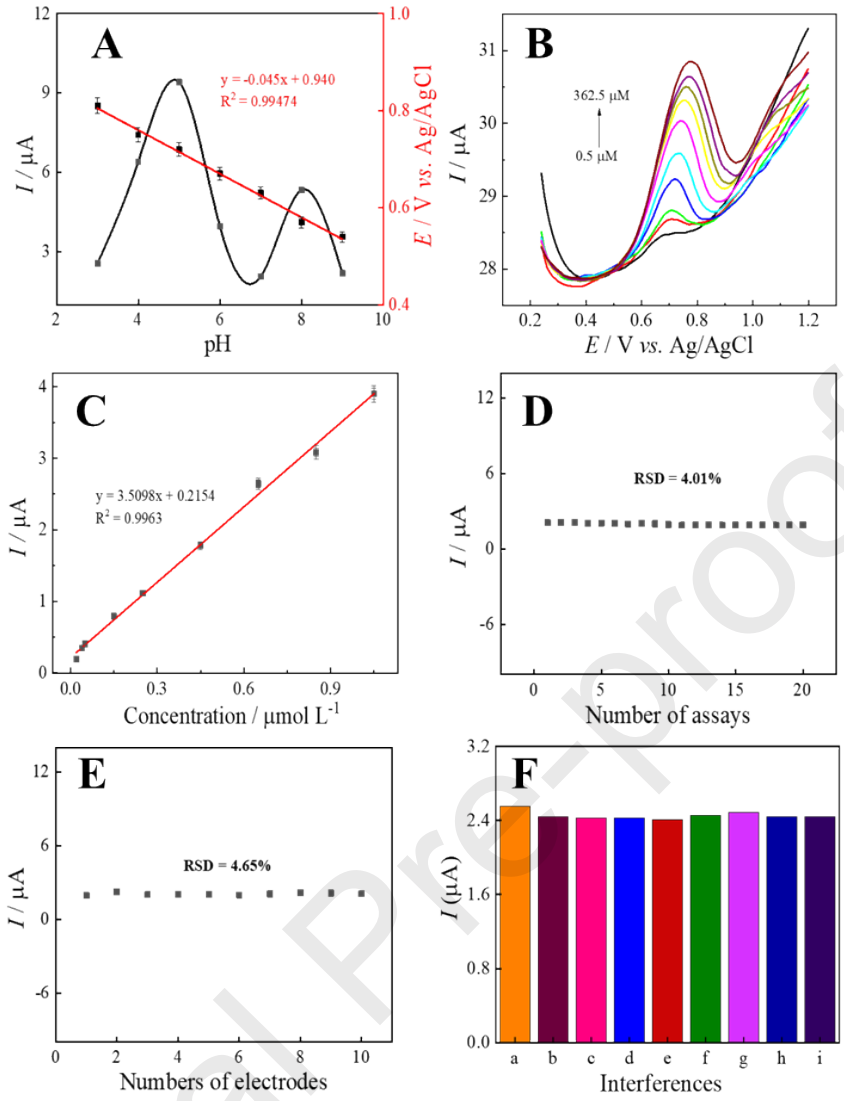

673

674 **Fig. 4.** (A) The effect of different pH on oxidation peak potentials (straight line) and
675 oxidation peak current values (curve) for SMZ in 0.04 M BR with scan rate 100 mV s^{-1};
676 (B) DPV of SMZ at h-BN/LIPG$_0$ electrode in 0.04 M BR containing concentration
677 from 0.5 - 362.5 μM at h-BN/LIPG$_0$ electrode; (C) The linear equation of SMZ with
678 different concentration from 0.5 - 36.25 μM; repeatability (D) and reproducibility (E)
679 of h-BN/LIPG$_0$ electrode for the determination of 5 × 10^{-5} mol/L SMZ in BR (pH
680 5.0); (F) Adding SMZ (a), NaCl (b), KCl (c), $MgCl_2$ (d), $CaCl_2$ (e), glucose (f),
681 glutamic acid (g), arginine (h) and hypoxanthine (i) in order in the same buffer to
682 study the effect of possible interfering substances on SMZ detection.

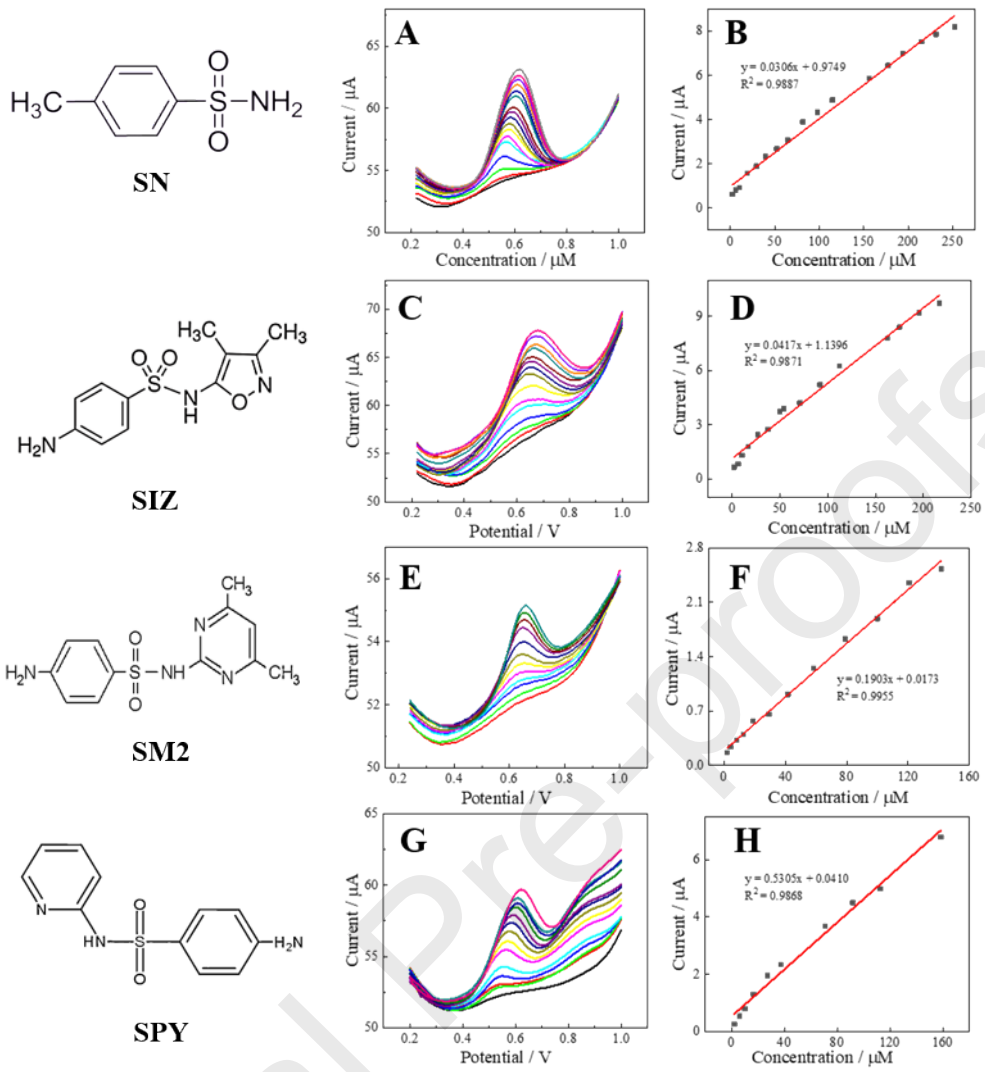

683

684 **Fig. 5** The proposed wireless and flexible electrochemical sensor based on
685 smartphone for the detection of four SAs with linear concentration range of 2.08 μM
686 to 233.33 μM and corresponding linear relationships: SN (A, B), SIZ (C, D), SM2 (E,
687 F), SPY (G, H).

688

689

690 **Table 1**. Recoveries obtained from real samples with the added SMZ using portable
691 sensor and HPLC method.

Name	Spiked	Portable sensor	HPLC method

	(μM)	Found [a] (μM)	RSD (%)	Recovery (%)	Found [a] (μM)	RSD (%)	Recovery (%)
Milk	0.00	N. D	-	-	N. D	-	-
	27.50	27.01 ± 0.036	1.96	98.2	29.56 ± 0.031	1.97	107.5
	55.00	55.71 ± 0.017	2.11	101.3	59.51 ± 0.056	1.05	108.2
Lake water	0.00	N. D	-	-	N. D	-	-
	27.50	26.81 ± 0.023	2.91	97.5	28.32 ± 0.004	2.13	103.0
	55.00	54.39 ± 0.085	3.08	98.9	54.56 ± 0.012	2.01	99.2

[a] Average value of three determinations ± relative deviation, N.D: Not detected.

Author statement

Manuscript title: MICROC-D-22-01014

I have made substantial contributions to the conception or design of the work; or the acquisition, analysis, or interpretation of data for the work; AND

I have drafted the work or revised it critically for important intellectual content; AND I have approved the final version to be published; AND

I agree to be accountable for all aspects of the work in ensuring that questions related to the accuracy or integrity of any part of the work are appropriately investigated and resolved.

All persons who have made substantial contributions to the workreported in the manuscript, including those who provided editing and writing assistance but who are not authors, are named in the Acknowledgments section of the manuscript and have given their written permission to be named. If the manuscript does not include Acknowledgments, it is because the authors have not received substantial contributions from nonauthors.

Attachment: Yes √No

Yifang Zeng

August 11, 2022

Declaration of interests

☑ The authors declare that they have no known competing financial interests or personal relationships that could have appeared to influence the work reported in this paper.

☐ The authors declare the following financial interests/personal relationships which may be considered as potential competing interests:

Scheme 1. Schematic illustration of the prepared of home-made integrated h-BN/LIPG$_0$ electrode and as a smartphone-based wireless platform for portable and fast detection of sulfonamides.

731

732

Highlights

- A laser-induced porous graphene as integrated flexible three-electrode was developed;
- A hexagonal boron nitride modified porous graphene as working electrode was developed;
- Smartphone-based wireless and flexible electrochemical sensor for sulfonamides was developed;
- A portable method for outdoor sensing was developed using the home-made integrated flexible three-electrode.

742

743